Food Chemistry 439 (2024) 138231

Contents lists available at ScienceDirect

Food Chemistry

journal homepage: www.elsevier.com/locate/foodchem

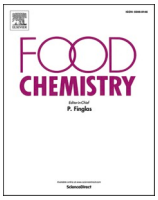

The addition of polysaccharide gums to *Aronia melanocarpa* purees modulates the bioaccessibility of phenolic compounds and gut microbiota: A multiomics data fusion approach following *in vitro* digestion and fermentation

Merve Tomas [a,1], Pascual García-Pérez [b,c,1], Araceli Rivera-Pérez [d], Vania Patrone [b], Gianluca Giuberti [b], Luigi Lucini [b,*], Esra Capanoglu [e]

[a] Department of Food Engineering, Faculty of Engineering and Natural Sciences, Istanbul Sabahattin Zaim University, 34303 Halkali, Istanbul, Turkey
[b] Department for Sustainable Food Process – DiSTAS, Università Cattolica del Sacro Cuore, Via Emilia Parmense 84, 29122 Piacenza, Italy
[c] Universidade de Vigo, Nutrition and Bromatology Group, Department of Analytical Chemistry and Food Science, Instituto de Agroecoloxía e Alimentación (IAA) – CITEXVI, 36310 Vigo, Spain
[d] Research Group "Analytical Chemistry of Contaminants", Department of Chemistry and Physics, Research Centre for Mediterranean Intensive Agrosystems and Agrifood Biotechnology (CIAIMBITAL), Agrifood Campus of International Excellence (ceiA3), University of Almeria, 04120 Almeria, Spain
[e] Department of Food Engineering, Faculty of Chemical and Metallurgical Engineering, Istanbul Technical University, 34469 Maslak, Istanbul, Turkey

ARTICLE INFO

Keywords:
Food matrix
Interaction
Phenolic metabolites
Bioaccessibility

ABSTRACT

This study aimed to determine how the addition of gellan, guar, locust bean, and xanthan gums affected the polyphenol profile of *Aronia melanocarpa* puree and the human gut microbiota after *in vitro* gastrointestinal digestion and large intestine fermentation. The different gums distinctively affected the content and bioaccessibility of phenolics in *Aronia* puree, as outlined by untargeted metabolomics. The addition of locust bean gum increased the levels of low-molecular-weight phenolics and phenolic acids after digestion. Gellan and guar gums enhanced phenolic acids' bioaccessibility after fermentation. Interactions between digestion products and fecal bacteria altered the composition of the microbiota, with the greatest impact of xanthan. Locust bean gum promoted the accumulation of different taxa with health-promoting properties. Our findings shed light on the added-value properties of commercial gums as food additives, promoting a distinctive increase of polyphenol bioaccessibility and shifting the gut microbiota distribution, depending on their composition and structural features.

1. Introduction

The food market is a highly growing competitive market for which consumer choice, purchasing patterns, and consumption behaviors are of critical importance. Therefore, food product development meeting consumer demands is necessary for food companies to survive in today's turbulent markets (Isaías et al., 2023). In the same way, the current trends in the global food market highlight a growing general interest in the consumption of natural-based functional foods with associated health-promoting properties, although several authors have claimed about the importance of determining the bioaccessibility of bioactive compounds to provide a realistic insight about their reliable effect on the human body (Thomson et al., 2021; Rainero et al., 2022). Thus, an increasing number of research studies have focused on the importance of deciphering the implications ascribed to the interactions between polyphenols and macromolecules in foods, since phenolic-rich foods are usually consumed along with macronutrients, such as carbohydrates, proteins, and fats, leading to inevitable interactions between macronutrients and polyphenols, influencing their gastrointestinal fate (Liu et al., 2021). These interactions could either show synergistic or antagonistic effects on the bioactivity of polyphenols and, consequently, exhibit significant nutritional implications attributed to their consumption (Rocchetti et al., 2022; Tomas, 2022).

Aronia or black chokeberry (*Aronia melanocarpa*) is one of the richest

* Corresponding author.
E-mail address: luigi.lucini@unicatt.it (L. Lucini).
[1] These authors contributed equally to this work and are the co-first authors.

https://doi.org/10.1016/j.foodchem.2023.138231
Received 28 September 2023; Received in revised form 11 December 2023; Accepted 15 December 2023
Available online 17 December 2023

sources of bioactive compounds, especially anthocyanins, comparable to berries. It is seldom consumed as fresh due to its astringent taste, but it can be easily added to different foods and beverages or as a supplement or food colorant. Aronia fruit and its products have great health-promoting activities, related to their high phenolic contents, which are represented by a wide range of polyphenols, especially phenolic acids and flavonoids (Sidor & Gramza-Michałowska, 2019).

Dietary fiber is an important functional ingredient with relatively great levels in plant-based foods. Gums, a soluble dietary fiber, belong to the class of polymers that are water soluble and form a viscous structure. Besides their biological functions, dietary fibers also play an important role in food products' sensory and textural characteristics (Mudgil & Barak, 2019). Moreover, dietary fibers significantly improve gut microbiota balance and human health. Although polyphenols bound to fiber are not digested in the small intestine, they could be released by microbial fermentation in the large intestine. Thus, released phenolic compounds can exert beneficial health effects at the site. These fermentable dietary fibers can act as prebiotics that stimulate the growth of beneficial gut microbiome, contributing to various health effects (Thomson et al., 2021). In this sense, Loo et al. (2023) recently reported that combining polyphenol-rich sugarcane extract and fiber could increase phenolic compounds' availability in the colon and modulate the gut microbiota towards a more favourable profile. Nevertheless, the great impact of fermentable fibers on the shift of gut bacterial communities is difficult to predict in terms of health-promoting effects since a high number of heterogeneous taxa is directly affected by the presence of these polysaccharides (Naimi et al., 2021). Consequently, much attention is required to evaluate and further reveal the potential of dietary fiber supplementation on the enhancement of bioactive properties during the design of novel functional foods.

In the present study, four types of commercial gums with different origins and structural conformations were subjected to the enrichment of Aronia puree, i.e.: (i) gellan gum, an ionic microbial exopolysaccharide from *Sphyngomonas elodea* with linear structure, formed by three different residues, i.e.: glucose, glucuronic acid, rhamnose in a ratio 2:1:1 (Das & Giri, 2020); (ii) guar gum, a non-ionic plant-derived polysaccharide with a branched conformation of galactomannan as the basic skeleton with branches of galactose residues, resulting in a ratio mannose:galactose of 2:1 (Viuda-Martos et al., 2018); (iii) locust bean gum, a non-ionic plant-derived polysaccharide with linear structure similar to that of guar gums but with a different mannose:galactose ratio, 4:1 (Naimi et al., 2021); and (iv) xanthan gum, an ionic microbial exopolysaccharide from *Xanthomonas campestris* with helicoidal conformation, composed of glucose, mannose, and glucuronic acid with the molar ratio 2:2:1 (Abu Elella et al., 2021). A combined untargeted metabolomics approach with gut microbiota metagenomics will be carried out to decipher the effect of gum enrichment on the phenolic compounds bioaccessibility and gut microbiota distribution of Aronia puree following a simulated *in vitro* gastrointestinal digestion and *in vitro* large intestine fermentation.

2. Materials and methods

2.1. Aronia puree material

Raw *Aronia* fruit samples were obtained from a local shop in Turkey and defrosted at room temperature and ground in a Thermomix laboratory grinder for 5 min. Four different commercial gums, including (i) gellan gum (Kelcogel F, CPKelco, USA), (ii) guar gum (Alfasol, Turkey), (iii) locust bean gum (Alfasol, Turkey), (iv) xanthan gum (Alfasol, Turkey) were added at 1% (w/w) concentration. After the addition of gums, the *Aronia* puree was homogenized at 25,000 × *g* using a homogenizer (IKA T18 basic, Germany). Thereafter, the interaction between *Aronia* polyphenols and soluble dietary fiber was achieved by incubating samples at 35 °C in a shaker at 170 rpm for 30 min. The samples were prepared in three batch replicates.

2.2. In vitro human gastrointestinal digestion and large intestine fermentation

A standardized 3 step static *in vitro* human gastrointestinal digestion model was used (Minekus et al., 2014). The detailed procedure, along with all the procedural schemes, are fully described elsewhere (García-Pérez et al., 2024; Minekus et al., 2014). After 242 min of incubation, the *in vitro* digestion was stopped by ice bath cooling and the liquid fractions and solid residues were obtained after centrifugation at 4000*g* for 14 min at 4 °C.

The collected solid residues were then subjected to an *in vitro* large intestine fermentation (García-Pérez et al., 2024; Pérez-Burillo et al., 2021) using feces from three healthy adults who were not treated with antibiotics. The CO_2-saturated fermentation medium contained 32% wt/vol of fresh feces obtained by pooling equal amounts (wet weight) of feces from each subject. The *in vitro* fermentation step lasted 20 h at 37 °C under gentle oscillation under continuous CO_2 flushing (technical grade: 5.5; SAPIO, Monza, Italy) (Pérez-Burillo et al., 2021). At the end of the *in vitro* fermentation, samples were centrifuged at 4000*g* for 12 min and supernatants and solid residues were collected and stored (−40 °C). Informed written consent was obtained from all subjects, and the study was conducted in conformity with the Helsinki Declaration.

2.3. Extraction and spectrophotometric analyses of Aronia samples

Aronia samples, both the fresh samples and the puree, were extracted in triplicate by mixing 2 g of fresh samples with 5 mL of 75% aqueous methanol (*v/v*) acidified 0.1% formic acid (*v/v*) in a cooled ultrasonic bath for 15 min (Capanoglu et al., 2008). These were subsequently centrifuged at 2700*g* at 4 °C for 10 min, after which the supernatants were collected. This extraction procedure was repeated once more with the pellets, and both supernatants were pooled to reach a final volume of 10 mL. These extracts were stored at −20 °C until analysis. Total soluble phenols (TSP) were determined according to the Folin-Ciocalteu method reported by Singleton and Rossi (1965). Briefly, 0.75 mL of 10% Folin-Ciocalteu solution was added to 100 μL of the sample. After 5 min, 0.75 mL of 6% Na_2CO_3 solution was added, the mixture was shaken using a vortex and then kept in the dark for 90 min. After that, TSP was determined by measuring the absorbance in a spectrophotometer at 725 nm. The results were expressed as mg of gallic acid equivalent (GAE) per 100 g fresh weight (fw) of the sample. The total antioxidant capacity (TAC) assay was performed by cupric ion reducing antioxidant capacity (CUPRAC) method of Apak et al. (2004). Briefly, 100 μL of extract was mixed with 1 mL of 0.01 mM copper(II) chloride solution, 7.5 mM neocuproine and 1 M ammonium acetate (pH: 7). Immediately, 1 mL of distilled water was added to the mixture so as to make the final volume 4.1 mL. After 30 min of incubation at room temperature, absorbance was measured at 450 nm. The results were expressed as mg trolox equivalents (TE) per 100 g fw sample. The monomeric anthocyanin (TMA) content was determined colorimetrically by the pH differential method (Lee et al., 2005) and expressed in milligrams of cyanidin-3-*O*-glucoside equivalent (C3GE) per 100 g fw sample. Absorbance was measured at 520 and 700 nm in buffers at pH 1.0 (KCl, 0.025 M) and pH 4.5 (CH_3CO_2Na, 0.4 M) and calculated using Equation:

$$\mathrm{TMA} = \frac{(\mathrm{A\ x\ MW\ x\ DF\ x\ 1000})}{(\varepsilon\ \mathrm{x}\ 1)}$$

where A = (A520 nm–A700 nm) pH 1.0–(A520 nm–A700 nm) pH 4.5; MW = molecular weight of cyanidin-3-*O*-glucoside (C3G) (449.2 g/mol); DF = dilution factor; ε = molar extinction coefficient of C3G (26,900 L/(mol.cm)); and l = pathlength (cm).

2.4. Sample preparation and phenolic profiling via UHPLC-QTOF-HRMS untargeted metabolomics

Fresh raw *Aronia* samples from both puree and fruit were lyophilized, and 100 mg of dried samples were extracted with 1 mL of 80% (*v/v*) aqueous methanol acidified with 0.1% (*v/v*) formic acid. Afterward, samples were vortexed for 1 min at room temperature and subjected to ultrasound-assisted extraction using an ultrasonic bath for 30 min. For *in vitro* digested samples, the liquid fractions were lyophilized, and 100 mg of dried residue was resuspended in 1 mL of deionized water and vortexed for 1 min at room temperature. For fermented samples, 4 mL of liquid fermented solution was collected. All samples were centrifuged at 4 °C for 10 min at maximum speed (5810R centrifuge from Eppendorf®) and 1 mL of supernatants was collected and further filtered (0.22-μm pore size syringe filters) and placed into amber vials stored at −20 °C until analysis. A quality control sample (QC) was performed for raw, *in vitro* digested, and *in vitro* fermented samples by pooling 20-μL aliquots of each sample.

The phenolic profiling of *Aronia* samples was achieved by an untargeted approach through ultra-high performance liquid chromatography coupled with quadrupole-time-of-flight high-resolution mass spectrometry (UHPLC-QTOF-HRMS; G6550, Agilent). Chromatographic conditions consisted of an RP Poroshell 120 PFP column (2.1 × 100 mm, 1.9 μm particle size, Agilent) as stationary phase and a binary mobile phase including water as solvent A and acetonitrile as solvent B, being both acidified with 0.1% (*v/v*) formic acid. A gradient elution was performed starting from 94% A to 6% A for 32 min; the flow rate was 0.2 mL min^{-1} and the injection volume was 6 μL. The mass spectrometer electrospray ionization source was adjusted in positive mode, and nitrogen was used as sheath gas (12 L min^{-1} flow rate, 315 °C) and drying gas (14 L min^{-1} flow rate, 250 °C). Nebulizer pressure was adjusted at 45 psi, nozzle voltage at 350 V, and capillary voltage at 4000 V. The high-resolution mass acquisition was performed in full scan mode at *m/z* range of 100–1200 (1 spectrum per second) with 30,000 FWHM resolution. All samples were analyzed in triplicate, following a random injection course against a methanolic blank.

2.5. Data processing and semi-quantification of phenolic compounds

Following acquisition, the processing of metabolomic raw data was performed by MassHunter Profinder software (Agilent®). The "find-by-formula" algorithm was applied, and peak finding was obtained by the alignment of retention time, within the range 1–32 min with a tolerance of 0.05 min, and mass features, within the range 100–1200 *m/z* with a tolerance of 5 ppm. Data reduction was performed by selecting only the features annotated in at least 80% of replicates belonging to the same experimental group. The annotation of features was achieved by the accurate mass determination from full-scan MS data using the database Phenol-Explorer 3.6 (available at phenol-explorer.eu), and taking into account the monoisotopic accurate mass, isotopic pattern, and isotopic accurate spacing. Annotation was in compliance with level 2 of identification from the Metabolomics Standard Initiative (MSI): putatively annotated compounds.

The semi-quantification of phenolic compounds was achieved by their classification into several classes and subclasses, which were then quantified according to a representative analytical standard (all prepared and analyzed as described earlier for *Aronia* samples): cyanidin was selected as the reference standard of anthocyanins, (+)-catechin for flavanols, luteolin for flavones, chalcones, isoflavonoids and flavanones, quercetin for flavonols, sesamin for lignans, ferulic acid for phenolic acids, and tyrosol for tyrosols and other low-molecular-weight phenolics (LMW). The results for the quantification of flavonoid classes were combined. Results were expressed as the mean ± standard deviation in μg of standards equivalents per gram of dry matter (μg g^{-1}DM) for each phenolic class: flavonoids, lignans, LMW, and phenolic acids.

2.6. Metagenomic analysis of fecal inoculum

16S rRNA gene amplicon sequencing was used to analyze the bacterial profile of human fecal microbiota after *in vitro* fermentation of gum-added *Aronia* puree. For that purpose, bacterial pellets were obtained after centrifugation (12,000 × *g*, 10 min at 4 °C) of 2 mL-samples of fermentation suspensions and immediately frozen at −40 °C (Pérez-Burillo et al., 2021). For DNA extraction, the Fast DNA™ SPIN Kit for Soil (MP Biomedicals, Santa Ana, CA) and the FastPrep®-24 Instrument were used according to the manufacturer's instructions with minor modifications. DNA was checked by agarose gel electrophoresis to determine the quality and by Qubit HS dsDNA fluorescence assay (Life Technologies, Carlsbad, CA, USA) to estimate concentration. PCR amplification was performed with 10 ng of input DNA, 0.5 μM of each custom barcoded 341F (5′-CCTACGGGNGGCWGCAG-3′) and 805R (5′-GACTACHVGGGTATCTAATCC-3′) primer (targeting the V3-V4 hypervariable region of the 16S rRNA gene), and 1 × KAPA HiFi HotStart ReadyMix (Kapa Biosystems, Wilmington, MA, USA). Thermal cycling conditions were described elsewhere (Patrone et al., 2018). PCR amplicons of ~550 bp were quantified by Qubit HS dsDNA fluorescence assay and pooled in equimolar ratios. The final pool was purified with the Agencourt® AMPure® XP kit (Beckman Coulter, Italy, Milano). Library preparation and Illumina sequencing were performed at Fasteris/Gene Support SA (Plan-les-Ouates, Switzerland) using MiSeq v3 platform (https://www.illumina.com/) in a 2x300bp mode, following a previously described analysis pipeline (Miragoli et al., 2021). After sequencing, reads were demultiplexed based on their unique barcodes using Fasteris proprietary software, trimmed and overlapped by means of the Trimmomatic R package version 0.32 and Fastq processing command line tool *ea-utils* version 1.1.2 (https://expressionanalysis.github.io/ea-utils/). Reads were aligned to the reference database Silva138-SSU rRNA version SSURef_NR99_138_tax_silva_DNA.fasta using the mapping software Burrows-Wheeler Alignment Tool version 0.7.5a (https://bio-bwa.sourceforge.net/). The *samtools* were used to compute the number of reads mapped onto each OTU.

2.7. Statistical analysis

The generated data from the metabolomics approach were analyzed by the Mass Profiler Professional software (Agilent®). Firstly, the abundance of annotated compounds was normalized at the 75th percentile, log_2-transformed, and baselined against the median values of all samples. An unsupervised hierarchical cluster analysis (HCA) was performed to establish the similarities and/or differences between samples according to their phenolic profile (Euclidean distance, Ward's linkage rule). Then, a fold-change (FC) analysis and analysis of variance (ANOVA) were performed to statistically determine the effect of different gums on the abundance of annotated compounds (logFC cut-off = 2; statistical significance, $\alpha = 0.05$). Moreover, a supervised orthogonal projection to latent structures discriminant analysis (OPLS-DA) was performed to predict the discrimination by means of phenolic profiling due to the application of different gums by SIMCA 16 software (Umetrics®) on raw, digested, and fermented *Aronia* samples. The quality of OPLS models was evaluated by high values of goodness-of-fit and predictability parameters (R^2 and Q^2, respectively), after developing their statistical validation through cross-validation ANOVA and refuting the overfitting through permutation test (n = 100). The OPLS analysis was combined with a variable importance in projection (VIP) analysis to identify those compounds with the highest discrimination in the prediction models, called VIP markers, which were classified according to their VIP score (VIP score threshold = 1.1). On the other hand, the results proceeding from the semi-quantification of phenolic compounds were analyzed by the SPSS 25 (IBM®) statistical software through one-way ANOVA ($\alpha = 0.05$) followed by Duncan's *post hoc* test (n = 6).

Data obtained from 16S rRNA amplicon metagenomic sequencing

were analyzed by the R package *vegan*, version 2.3–3. The original abundance matrix was rarefied to the smallest library size to standardize sample raw read counts before diversity analysis. The impact of gum addition on the richness and evenness of fecal bacterial communities was estimated by calculating Chao1 and Shannon indexes, and ANOVA was used to compare the effect of different gums on α-diversity. Bray-Curtis dissimilarity was used to estimate β-diversity, and permutational multivariate analysis of variance (PERMANOVA) was used to assess significance levels of compositional differences in β-diversity among microbial populations. To identify bacterial taxa that were more/less abundant in each group, the *metacoder* R package was applied as incorporated in the MicrobiomeAnalyst platform (https://www.microbiomeanalyst.ca/MicrobiomeAnalyst/home.xhtml). This method relies on the hierarchical structure of taxonomic classifications to quantitatively and statistically illustrate taxonomic differences between microbial communities.

2.8. Integration of metabolomic and metagenomic output datasets via multi-omics approach

The output datasets from both metabolomics and 16S rRNA gene amplicon sequencing metagenomics, including those at family, genus, and species levels were jointly analyzed using the Data Integration Analysis for Biomarker discovery using Latent variable approaches for Omics studies (DIABLO) framework available from the "mixOmics" package (version 6.22) in R software (version 4.2.1.). Firstly, three independent (sparse) Partial Least Squares (s)PLS models were performed to calculate the correlation between metabolomics and metagenomics datasets. Afterward, DIABLO modeling, based on multiblock (s)PLS discriminant analysis ((s)PLS-DA) was carried out to assess the determined correlations at the component level of the tested treatments. For this purpose, the DIABLO model was optimized by applying the tuning function in terms of the number of components, selecting those achieving the lowest overall balanced error rate and using the centroid distance to give the best accuracy, and the number of variables to select in each dataset, by performing a repeated 10-fold stratified cross-validation.

3. Results and discussion

3.1. Spectrophotometric analyses of Aronia samples: Total soluble phenols, total antioxidant capacity, and total monomeric anthocyanin content

The total soluble phenols (TSP), total antioxidant capacity (TAC), and total monomeric anthocyanin content (TMA) of *Aronia* samples are given in Table 1. In *Aronia* fruit, TSP, TAC, and TMA levels were 930.4 mg GAE, 1307.4 mg TE, and 107.9 CGE per 100 g fw, respectively. After puree processing, TSP, TAC, and TMA values were not significantly decreased, as reported for the control, but puree supplementation with guar gum, locust bean gum, and xanthan gum showed significant decreases of 21%, 28%, and 41% in TSP, respectively as compared to the control ($p < 0.05$). Similarly, TAC values significantly decreased by 24%, 22%, and 27% when guar gum, locust bean gum, and xanthan gum were added to the puree, respectively ($p < 0.05$). However, adding gellan gum to *Aronia* puree did not significantly change the TSP and TAC levels. Furthermore, with the addition of xanthan gum to *Aronia* puree, the TSP, TAC, and TMA values were observed to be the lowest. These results might be due to the differences in the interaction between gums and polyphenols. Consistent with these results, the incorporation of soluble fibers into blackberry puree (Tomas et al., 2020), and red raspberry puree (Tomas, 2022) resulted in significant losses in TSP, TAC, and TMA as compared to those of control samples ($p < 0.05$). Available literature shows that dietary fiber can directly interact with polyphenols, thereby preventing their action as antioxidants. Phenolic-dietary fiber interactions can be grouped as non-covalent interactions (reversible) and covalent interactions (mostly irreversible). Although van der Waals forces, electrostatic attraction, hydrophobic contact, or covalent bonding (esterification) interactions play a role, these interactions are mainly driven by the hydrogen bond (Rocchetti et al., 2022).

The impact of different gums on the gastrointestinal fate of *Aronia* samples was examined using a simulated gastrointestinal tract model (Table 1). *Aronia* puree processing showed significantly higher levels of TSP (21%) and TAC (13%) in the *in vitro* intestinal phase compared to the *Aronia* fruits ($p < 0.05$). On the other hand, TSP and TAC values of the intestinal phase decreased significantly in *Aronia* purees containing different gums (except gellan gum) compared to the control ($p < 0.05$). Bioaccessibility of TSP was significantly affected by the type of gums and reduced in the order of xanthan gum > locust bean gum > guar gum ($p < 0.05$). These findings could be explained by the interactions between gum and polyphenols and their entrapment within gum molecular structure, thus resulting in their decreased release within the intestinal phase. Our results also revealed that different types of gums in *Aronia* puree affected phenolics' content and bioaccessibility. The current observations were in line with Jakobek et al. (2022), who reported that the flavonol release was increased during oral, gastric and intestinal digestion, whereas phenolic acids and anthocyanins first increased in the gastric phase and then decreased in the intestinal phase, indicating the entrapment of phenolics by β-glucan in *Aronia* samples. The same researchers reported that the adsorption was affected by the initial concentration of polyphenols and β-glucan. It is also worth emphasizing that the structure, concentrations, and compositions of phenolic compounds and dietary fibers may influence their interactions, leading to differences in their physicochemical and functional attributes. Similarly, it has been reported that dietary fiber addition decreased the bioaccessible levels of TSP and TAC in blackberry (Tomas et al., 2020), red raspberry (Tomas, 2022) and cherry laurel purees (García-Pérez et al., 2024). The Folin-Ciocalteu method is used to estimate the amount of total soluble phenolics. However, it is essential to note that the assay is not specific

Table 1
Spectrophotometric determination of total soluble phenols (TSP), total monomeric anthocyanin content (TMA), and antioxidant capacity in terms of cupric reducing antioxidant capacity (CUPRAC) on *Aronia* samples.

	Levels	Fruit	Control	Gellan gum	Guar gum	Locust bean gum	Xanthan gum
TSP	Raw	930.4 ± 96.5 a	880.7 ± 75.5 a	797.1 ± 54.9 a	694.2 ± 28.5b	637.5 ± 16.4b	516.4 ± 19.8c
	Digested	452.6 ± 17.2b	546.8 ± 59.3 a	527.7 ± 38.1 a	463.8 ± 68.7b	505.1 ± 56.9b	498.8 ± 47.3b
TMA	Raw	107.9 ± 21.2 a	109.8 ± 40.5 a	112.0 ± 34.5 a	101.0 ± 41.1 a	109.1 ± 23.8 a	80.7 ± 19.5b
	Digested	9.4 ± 2.1 a	2.7 ± 1.8c	1.8 ± 0.7 d	0.4 ± 0.1 e	6.0 ± 0.3b	3.0 ± 0.1c
CUPRAC	Raw	1307.4 ± 78.4 a	1265.5 ± 46.9 a	1221.6 ± 33.8 a	962.5 ± 70.2b	985.2 ± 29.8b	929.9 ± 93.2b
	Digested	759.9 ± 65.0b	859.0 ± 51.0 a	843.6 ± 45.8 a	773.7 ± 87.6b	760.8 ± 97.7b	775.9 ± 45.1b

Data represent mean ± standard deviation (n = 6). Different letters within the same row indicate statistically significant differences ($p < 0.05$). TSP was expressed in mg GAE per 100 g of fresh weight (FW), TMA was expressed in mg CGE per 100 g FW, and CUPRAC was expressed as mg TE per 100 g FW.

for phenolic compounds, and other compounds, such as sugars, tryptophan, ascorbic acid, thiols, etc., have the potential to reduce the Folin reagent. Therefore, the possibility to have interfering compounds should be considered when interpreting this parameter (Castro-Alves & Cordenunsi, 2015; Everette et al., 2010). On the other hand, gellan gum and guar addition to the *Aronia* purees reduced TMA by 33–85%, while xanthan gum addition increased TMA by 22% in the intestinal phase ($p < 0.05$). The results of this study showed that gums can interact with polyphenols and thus significantly affect their bioaccessibility. Based on these findings, dietary fibers can act as an entrapping matrix, thereby limiting the bioaccessibility of flavonoids. It is also worth emphasizing that dietary fibers limit the bioaccessibility of phenolics in the small intestine, but they act as fermentative substrates for the microbial community in the colon (Thomson et al., 2021).

3.2. Phenolic profiling of gum-enriched Aronia samples during in vitro gastrointestinal digestion and fermentation via UHPLC-QTOF-HRMS untargeted approach

A total of 338 annotated features were obtained, and the full list of compounds is displayed in Table S1, including their classification within phenolic class and subclass, abundance, retention time (min), molecular mass (u), and molecular formula. The untargeted phenolic profile of *Aronia* samples contained: 42 anthocyanins, represented mainly by cyanidin glycosides; 18 flavanols, essentially including catechin-based compounds; 5 chalcones and dihydrochalcones, for instance, phloretin derivatives; 27 flavones, especially luteolin and apigenin glycosides; 14 flavanones, mainly containing naringenin and hesperidin glycosides; 18 isoflavonoids with a heterogeneous record; 22 flavonols, from which quercetin glycosides and derivatives covered the most of this subclass; 32 lignans, showing a diversified content; 65 LMW compounds, featuring alkylresorcinols, coumarins, and tyrosols; 79 phenolic acids and derivatives, mainly hydroxycinnamic acids; and 13 stilbenes (Table S1). The great variety of flavonoids and phenolic acids as the major constituents of *Aronia* fruits has been largely assessed in previous reports (Sidor & Gramza-Michałowska, 2019), although this is the first research providing a high-resolution metabolomic insight reporting stilbenes and LMW phenolics in this matrix.

Concerning the experimental design, three factors were involved in this research to determine the effect of gums in the bioaccessibility of *Aronia* polyphenols: *Aronia* matrix, including fruits and puree; three levels of digestion, considering raw, *in vitro* gastrointestinal digested samples, and *in vitro* fermented samples; and the addition of four different gums into *Aronia* puree. Due to the multifactorial design, an initial multifactorial approach was developed through an unsupervised hierarchical cluster analysis, HCA, to naively decipher the influence of different factors on the phenolic profile of *Aronia*. Firstly, HCA was performed to determine the similarities and differences between the two *Aronia* matrices and their digestion level (Fig. S1). The results indicated that the *in vitro* digestion played a pivotal role in the phenolic profile, whereas subtle differences were observed between the fruit and puree (Fig. S1). Indeed, an ANOVA was performed to statistically determine the compounds showing a significantly different abundance, and only 16 compounds were significantly different ($p < 0.05$) when considering the matrix effect (Table S2). Owing to this evidence, *Aronia* fruits exhibited a highly similar profile to puree; consequently, only puree will be considered in the subsequent analyses, as it was used as the control for the enrichment with gums. Moreover, to better evaluate the role of different gums in the bioaccessibility of *Aronia* puree polyphenols, the data derived from the metabolomics analysis were considered according to the different digestion levels, thus discriminating between raw, digested, and fermented samples. For the purpose following annotation, phenolic compounds were grouped and quantified according to a representative reference standard of each class, and results are shown in Table 2. In all cases, LMW represented the class with the highest content in *Aronia* samples (ranging 12.1–14.8 μg g^{-1}DM), followed by flavonoids (3.6–5.5 μg g^{-1}DM), phenolic acids (1.7–1.9 μg g^{-1}DM) and lignans (0.30–0.46 μg g^{-1}DM; Table 2).

Table 2
Semi-quantification of phenolic compounds annotated in *Aronia* extracts, expressed as the mean ± standard deviation (n = 6) in μg per gram of dry matter (μg/g DM).

Phenolic classes	Levels	Control	Gellan gum	Guar gum	Locust bean gum	Xanthan gum
Flavonoids	Raw	4.1 ± 0.13 bc	5.5 ± 0.23 a	4.4 ± 0.40b	3.6 ± 0.87c	4.6 ± 0.70b
	Digested	0.44 ± 0.12 a	0.37 ± 0.007 a	0.44 ± 0.11 a	0.33 ± 0.10 ab	0.23 ± 0.05b
	Fermented	0.32 ± 0.02 a	0.27 ± 0.03b	0.33 ± 0.03 a	0.33 ± 0.03 a	0.32 ± 0.02 a
	$\%BA_{dig}$	10.7 ± 2.8 a	9.2 ± 0.16 a	10.7 ± 2.6 a	8.0 ± 2.4 ab	5.6 ± 1.1b
	$\%BA_{ferm}$	7.9 ± 0.40 a	6.7 ± 0.80b	8.0 ± 0.74 a	8.1 ± 0.63 a	6.8 ± 0.62 a
Lignans	Raw	0.33 ± 0.06b	0.35 ± 0.05b	0.32 ± 0.04b	0.30 ± 0.03b	0.46 ± 0.03 a
	Digested	0.23 ± 0.01 a	0.07 ± 0.004c	0.08 ± 0.01 bc	0.09 ± 0.01b	0.08 ± 0.01 bc
	Fermented	0.06 ± 0.01 a	0.05 ± 0.01b	0.06 ± 0.003 a	0.06 ± 0.01 ab	0.06 ± 0.003 a
	$\%BA_{dig}$	68.3 ± 2.7 a	20.4 ± 1.1b	24.3 ± 4.3b	27.8 ± 2.9b	24.1 ± 3.8b
	$\%BA_{ferm}$	17.3 ± 2.7 a	14.4 ± 2.3b	18.7 ± 0.74 a	16.5 ± 3.3 ab	17.2 ± 0.91 a
LMW	Raw	12.1 ± 3.9 a	14.8 ± 0.38 a	12.5 ± 0.43 a	13.2 ± 0.31 a	12.4 ± 2.7 a
	Digested	4.1 ± 0.61b	4.0 ± 0.40b	3.4 ± 0.97b	5.6 ± 0.26 a	4.4 ± 0.71b
	Fermented	2.8 ± 0.54 ab	3.3 ± 0.22 a	1.9 ± 0.40c	2.6 ± 0.49b	2.6 ± 0.32b
	$\%BA_{dig}$	33.7 ± 5.1b	32.4 ± 3.3b	28.5 ± 8.1b	46.3 ± 2.1 a	36.6 ± 5.9b
	$\%BA_{ferm}$	23.6 ± 4.5 ab	27.0 ± 1.8 a	15.4 ± 3.3c	21.3 ± 4.1b	21.5 ± 2.7b
Phenolic acids	Raw	1.9 ± 0.12 a	1.8 ± 0.08 a	1.7 ± 0.24 a	1.8 ± 0.18 a	1.8 ± 0.24 a
	Digested	0.37 ± 0.02c	0.34 ± 0.04c	0.45 ± 0.07b	0.59 ± 0.07 a	0.58 ± 0.04 a
	Fermented	0.14 ± 0.02b	0.27 ± 0.02 a	0.28 ± 0.02 a	0.15 ± 0.02b	0.16 ± 0.04b
	$\%BA_{dig}$	19.6 ± 1.1c	17.9 ± 1.9c	24.3 ± 4.0b	31.8 ± 3.9 a	30.8 ± 2.0 a
	$\%BA_{ferm}$	7.5 ± 1.0b	14.7 ± 1.3 a	14.7 ± 1.2 a	8.0 ± 1.1b	8.5 ± 1.9b

Different capital letters within the same row indicate significant differences according to Duncan's *post hoc* test ($p < 0.05$) for each treatment. $\%BA_{dig}$, percentage of bioaccessibility after *in vitro* gastrointestinal digestion; $\%BA_{ferm}$, percentage of bioaccessibility after fermentation.

Concerning raw materials, the application of gums did not play a significant role in the content of LMW and phenolic acids. In contrast, it was statistically significant in the case of flavonoids, where gellan gum enrichment provoked a significant 25.4% increase with respect to control. In contrast, the rest of the gums did not alter the flavonoid content

(Table 2). These results are in accordance with those of TMA (Table 1), suggesting the importance of anthocyanins within this phenolic class. Notably, the anionic nature of gellan gum makes this macromolecule an outstanding gelling agent whose hydrophilicity is enhanced in the presence of cations (Das & Giri, 2020), as is the case of anthocyanins. In turn, it was recently assessed that the solubility and stability of fruit-derived anthocyanins were improved in the presence of gellan gum (Wu et al., 2021), thus supporting present findings. Accordingly, focusing on the corresponding HCA, the unsupervised multivariate analysis suggested that adding gums impacts *Aronia* puree's phenolic profiling (Fig. 1A). In combination with HCA, the OPLS-DA model on raw samples allowed discriminating the metabolomic profile after the addition of different gums (Fig. 1B): guar and LB gums were grouped, indicating a very similar profile that can be assessed based on their non-ionic nature, whereas xanthan gum exhibited the most differential profile. This model was combined with a VIP analysis, indicating the compounds with the greatest influence in discrimination, which were mostly represented by flavonoids (34.5%), LMW (29.1%), and phenolic acids (25.5%; Fig. 1C). Among flavonoids, xanthan gum presented the strongest positive effect, as observed from their logFC values: 6.41 for the anthocyanin cyanidin 3-*O*-(6″-malonyl-glucoside) and the isoflavonoids 6″-*O*-acetylgenistin and 6″-*O*-malonylglycitin (Table S3). The complexation of anthocyanins by the anionic xanthan polysaccharide has been proven to be developed through strong hydrogen bonds and van der Waals forces, thus facilitating their stability and solubility (Zhao et al., 2021). In parallel, guar gum enrichment drove the accumulation of flavonoids with a high degree of glycosylation, as observed for kaempferol 3,7,4′-*O*-triglucoside and cyanidin 3-*O*-diglucoside-5-*O*-glucoside (logFC = 6.31 for all of them; Table S3), suggesting an enhanced association with these compounds. However, the performance of gums as flavonoid stabilizers is highly dependent on the composition and physicochemical properties of the original matrix, making difficult the definition of a particular outcome towards these polyphenols (Zhao et al., 2021). Besides flavonoids, discriminant LMW was represented by alkylphenols whose abundance was generally higher in the case of gellan, guar and LB gums, as shown for 5-heptadecylresorcinol (logFC = 6.31–6.91) and 5-nondecylresorcinol (logFC = 1.86–3.61), whereas 4-vinylsyringol was found accumulated (logFC = 6.41) only for xanthan (Table S3). In turn, the accumulation of tyrosols decreased in all cases. Such evidence suggests a high affinity of water-soluble gums towards 5-(*n*)-alkylresorcinols, as reported during the preparation of xanthan-loaded alkylresorcinols-enriched emulsions (Dey et al., 2013).

Considering the phenolic content of *Aronia* samples after *in vitro* gastrointestinal digestion, a significant decrease was observed in all classes. Among gums, gellan and guar gums showed a slightly similar profile, whereas LB and xanthan gums exhibited a common profile, according to both unsupervised (HCA) and supervised (OPLS) multivariate analyses (Fig. 1D and E, respectively). Indeed, the OPLS model generated indicates that gums played a role in the phenolic profile after digestion with respect to control (Fig. 1E). In quantitative terms, the similarities between LB and xanthan gums are shown through the TSP values since they promoted the highest rates for digested samples (Table 1). In the same way, the enrichment of *Aronia* puree with these gums reflected an enhancement in the bioaccessibility of the two most prevalent phenolic classes: LMW, increasing bioaccessibility to 46.3% for LB gum and 36.6% for xanthan gum and phenolic acids, whose

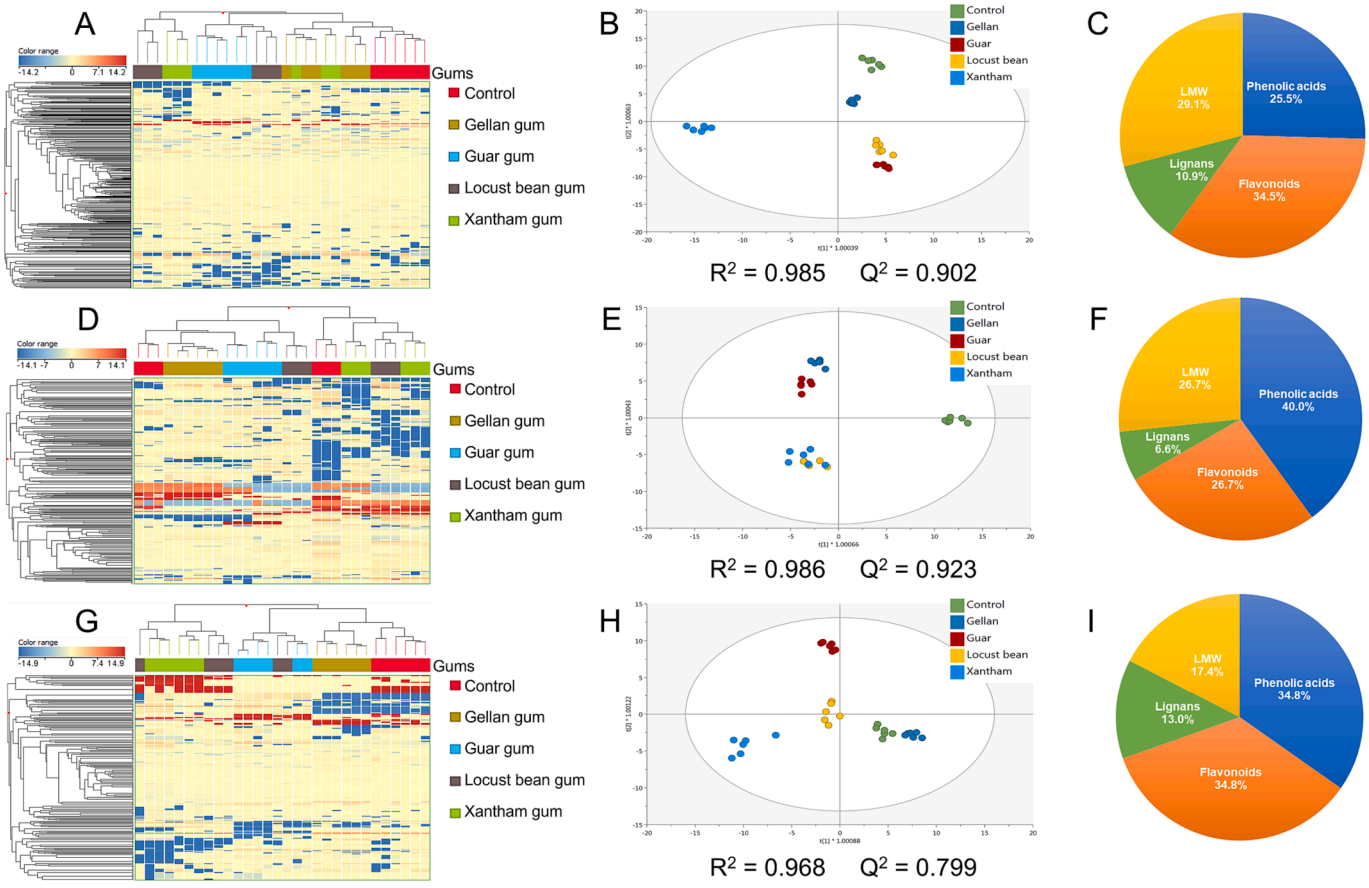

Fig. 1. Chemometrics analyses of *Aronia* puree samples. A–C. Raw samples; D–F. Digested samples; G–I. Fermented samples. Heatmap-based HCA (A, D, G) were obtained by the application of Euclidean distance and Ward's algorithm for log2-transformed, normalized abundances. The OPLS-DA models (B, E, H) present high-quality parameters, in terms of goodness-of-fit (R^2 = 0.968–0.986) and goodness-of-prediction (Q^2 > 0.799–0.923). The proportion of phenolic classes of the corresponding VIP markers (VIP score > 1.1) was displayed in graphic sectors (C, F, I).

bioaccessibility was increased up to 31.8% for LB gum and 30.8% for xanthan gum (Table 2). In contrast, for lignans and flavonoid contents, those gums promoted a decrease in gum-free puree, which was statistically significant ($p < 0.05$) in the case of xanthan (Table 2). Consequently, phenolic acids were predominantly spotted as VIP markers, representing 40% of all metabolites, followed by LMW and flavonoids (26.7% for each class; Fig. 1F). Regarding phenolic acids, a general accumulation of parental compounds and related catabolites was observed for all gums (Table S4). For instance, gallic acid (logFC = 2.43–5.74), *p*-coumaric acid 4-*O*-glucoside (logFC = 1.39–3.85), and ferulic acid 4-*O*-glucoside (logFC = −0.01–1.66) were suggested to be associated with gum, as well as their catabolites 4-hydroxyhippuric acid (logFC = 0.44–1.66), dihydrocaffeic acid 3-*O*-glucuronide (logFC = 0.15–2.10; Table S4). These results suggest a significant role of polysaccharide gums in protecting the integrity of phenolic compounds during gastrointestinal digestion, thus improving their bioaccessibility even under glycosylated forms. The carrier effect of phenolic acids attributed to gums along the gastrointestinal tract has been previously reported in maqui berry puree enriched with xanthan and guar gums (Viuda-Martos et al., 2018), in line with present findings. Indeed, xanthan gum has been characterized as a high-affinity carrier of phenolic acids, taking advantage of the preparation of health-promoting food preparations (Widelska et al., 2019). Interestingly, in the case of flavonoids, the addition of guar gum promoted the accumulation of flavonoids triglycosides (logFC = 8.14; Table S4), as stated above for raw samples, thus suggesting a protecting effect of guar gum towards these compounds during the *in vitro* digestion. This is an important outcome, as both xanthan and guar gums present helicoidal and highly-branched conformations, respectively, that prevent the access of degradation enzymes to the carried metabolites (Abu Elella et al., 2021; Grgić et al., 2020).

In the case of *in vitro* fermented samples, a slight effect of gums was observed in quantitative terms for all phenolic classes, except for phenolic acids, where gellan and guar gums promoted a significant increase in bioaccessibility from 7.5% in control to 14.7% in both cases (Table 2). It is worth mentioning that fermented samples were represented by the soluble fraction of fermentates, including the phenolic compounds released and metabolized after the fermentation, without considering those eventually linked to fiber that would be released. The HCA reflected a similar profile between gellan gum and the control, whereas LB gum showed an intermediate profile within guar and xanthan gums (Fig. 1G). This observation was thereafter confirmed by the corresponding OPLS model, conferring a close similarity between gellan gum and the control, whereas LB gum was spotted as intermediate to the rest of the gums (Fig. 1H). The anionic, low-branched linear structure of gellan (Sapper et al., 2019) was found to exert a less significant effect on the phenolic profile of fermented *Aronia* purees, thus reinforcing the hypothesis that spatial conformation is a paramount feature in the protecting effect of polysaccharide gums. In the same way, those gums with a complex spacial conformation (xanthan and guar) were grouped apart from the control, according to the same model (Fig. 1H), validating this hypothesis. Focusing on the proportion of VIP markers, phenolic acids and flavonoids were spotted as the most discriminant metabolites between treatments, accounting for up to 34.8% in both cases (Fig. 1I). Among flavonoids, there was an intense accumulation of flavonoid aglycones for LB and xanthan gums, reporting a logFC > 4.0 values for irilone, dihydroformononetin, and pelargonidin, whereas flavonoid glycosides showed a down-accumulation, as observed for xanthan gum (logFC = −1.24 and −6.37 for 6″-*O*-acetylglycitin and pelargonidin 3-*O*-arabinoside, respectively; Table S5). Concerning phenolic acids and their glycosides, a general decrease was observed following a gum-dependent trend (Table S5). Interestingly, some catabolites were also spotted as VIP markers, as is the case of the oxidized gallic aldehyde (logFC = −1.34–0.19) and 5-(3′-methoxy-4′-hydroxyphenyl)-γ-valerolactone (logFC = −2.45–0.54; Table S5). In general, gums differentially modulated the microflora-mediated catabolism of phenolic compounds. Among VIP markers, different levels of phenolic catabolites were spotted, as flavonoids were considered the most complex polyphenols analyzed. In this sense, several microorganisms from the human microbiota are responsible for the catabolism of phenolic compounds (Carregosa et al., 2022), which includes the production of flavonoids aglycones and dihydroflavonoids, represented by dihydroformononetin; 5-(phenyl)- γ-valerolactones and valeric acids from different flavonoid scaffolds, such as 5-(3′-methoxy-4′-hydroxyphenyl)-γ-valerolactone; also, phenolic acids are suggested to proceed from either pre-existing compounds or from flavonoids catabolism, both being finally transformed into benzoic acids and benzenes (Carregosa et al., 2022), for instance, arbutin and oxidation products, such as the reported gallic aldehyde. As a whole, gum addition promoted a dual role in the phenolic profile of *Aronia* purees, acting as protectors of flavonoids and phenolic acids and modulating the microflora's metabolic performance by the polysaccharide nature of gums.

3.3. Impact of gum-enriched Aronia puree on human gut microbiota in vitro

The results of alpha and beta diversity analysis at the OTU level are shown in Fig. 2. Overall, the addition of different types of gum to *Aronia* puree had no significant effect on fecal bacterial richness ($p = 0.874$), whereas a significant decrease in evenness was observed for bacterial populations exposed to xanthan gum ($p < 0.001$). Beta diversity analysis revealed a significant impact of xanthan, guar, gellan and locust bean gums on microbiota composition relative to control samples (PERMANOVA, $p = 0.001$), as indicated by Bray-Curtis distances (Fig. 2). PCoA plot showed that gellan gum samples grouped closely with controls, whereas locust bean samples clustered closely with guar gum samples. Xanthan gum samples clustered separately, showing a more dispersed distribution. Overall, these findings indicate a wide and diversified ability of specific polysaccharide gums to affect fecal microbial communities, as expected based on their different chemical composition and structure.

Data analysis revealed that genera *Dialister*, *Roseburia*, *Ruminococcus*, family *Veillonellaceae*, and species *Dialister invisus* showed a significantly higher relative occurrence in guar gum compared to control samples meanwhile a significant decrease in *Bacteroides vulgatus* was found (Fig. 2D). Some common effects among locust bean and guar gums could be foreseen based on their structural similarity; both are high molecular weight galactomannans whose main chain consists of (1 → 4) linked β-D-mannose residues and the side chain of (1 → 6) linked α-D-galactose. Guar gum specifically promoted the growth of *Dialister,* which can generate propionate from succinate, and propionic acid has emerged as a modulator of host physiology by exerting lowering effects on fatty acids and inflammation (Al-Lahham et al., 2010). Moreover, the anti-inflammatory effects of guar gum have been demonstrated in several murine experimental models, though disease protection appeared to be independent of alterations to the microbiota induced by the fiber (Fettig et al., 2022).

Gellan gum addition resulted in the down-regulation of several taxa, including genera *Dorea*, *Erysipelotrichaceae_UCG_003* and *Faecalibacterium*, species *Ruminococcus bicirculans*, family *Erysipelatoclostridiaceae* (Fig. 2E). However, it had a minimal effect on fecal community structure; this result was expected since the soluble fiber gellan is known to be poorly fermented by microorganisms, although soluble fibers are generally more rapidly fermented than insoluble fibers (Thomson et al., 2021). Recently, gellan gum was reported to improve non-alcoholic fatty liver disease in mice by modulating the gut microbiota and metabolites (Do et al., 2023). However, the depletion of butyrate-producing bacteria like *Erysipelatoclostridiaceae* and *Faecalibacterium* observed in this study, the latter including the species *Faecalibacterium prausnitzii* with established anti-inflammatory properties (Lenoir et al., 2020), warrant further investigation to ascertain the actual impact of these microbial changes on human gut physiology.

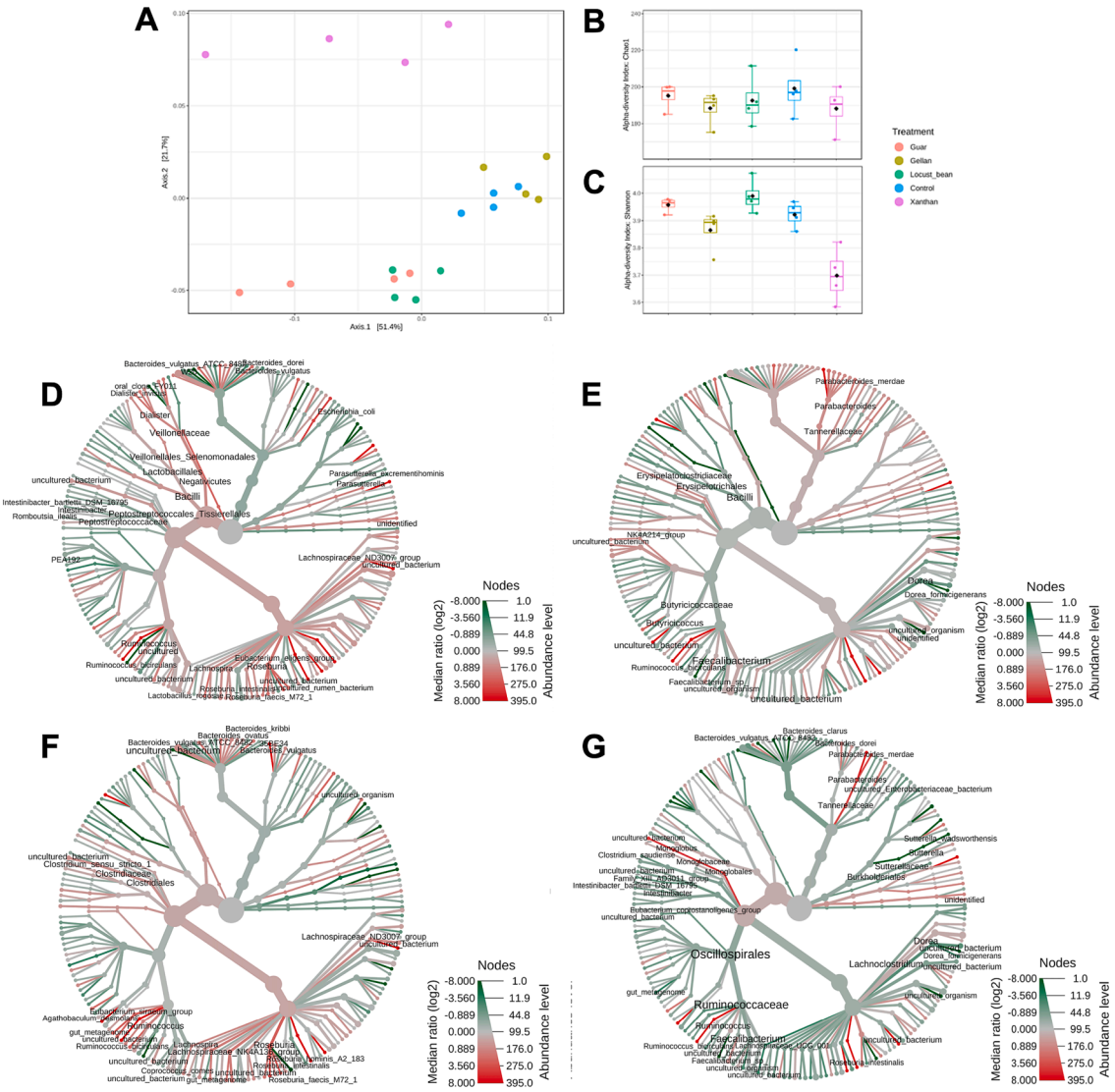

Fig. 2. Diversity of fecal bacterial communities after *in vitro* digestion and fermentation of *Aronia* puree supplemented with different polysaccharide gums. A. Principal Coordinate Analysis (PCoA) plot based on Bray Curtis dissimilarity metrics; percentage of variance explained by each axis is denoted in the corresponding axis label; B–C. Boxplots of Chao1 and Shannon diversity indexes, respectively. D–G. Metacoder heat trees showing pairwise comparisons of fecal communities composition between the different gum supplementation treatments and control, i.e.: guar gum (D), gellan gum (E), locust bean gum (F), and xanthan gum (G), respectively. Red taxa are enriched while green taxa are depleted in treated samples vs control, as determined by Wilcox rank-sum test followed by Benjamini-Hochberg (FDR) correction for multiple testing. (For interpretation of the references to colour in this figure legend, the reader is referred to the web version of this article.)

Taxa assigned to genera *Roseburia*, *Ruminococcus*, *Lachnospiraceae*_NK4A136_group, species *Roseburia intestinalis* and *Ruminococcus bicirculans* were significantly more abundant in locust bean gum samples compared to control (Fig. 2F), while genus *Collinsella* (family *Coriobacteriaceae*) was significantly less abundant. A notable feature of the microbiota response to locust bean gum addition is the significant increase in bacterial taxa representing major acetate and butyrate producers in the human gut (Ma et al., 2020). Microbiota-derived short-chain fatty acids (SCFAs) play a crucial role in maintaining host digestive health by providing energy to colonic cells, promoting gut barrier impermeability, and regulating the body's immune system and inflammation. Remarkably, studies in rodents have demonstrated that an increase in the *Lachnospiraceae* NK4A136 group following bilberry anthocyanin extract (Li et al., 2019), is related to a reduction of intestinal inflammatory responses. On the other hand, the gut bacteria genus *Collinsella* was found to induce the expression of Th17 regulatory network cytokines and increase gut permeability (Chen et al., 2016), suggesting that the expansion of this genus may promote pro-inflammatory conditions in the human intestine.

Notably, the addition of xanthan gum exerted the strongest impact on fecal microbiota composition, resulting in the highest number of differentially abundant taxa when compared to control after fermentation (Fig. 2A – 2C). More specifically, xanthan gum significantly increased the levels of genera *Monoglobus* and *Parabacteroides* (species *Parabacteroides merdae*) and families *Monoglobaceae* and *Tannerellaceae*. *Monoglobus pectinilyticus* is the only representative of the genus *Monoglobus* so far (Fig. 2G); it has been described as a pectin-degrading specialist, equipped with a unique set of genes encoding carbohydrate-active enzymes and cell-surface S-layer homology domain-containing proteins (Kim et al., 2019). In line with these findings, enrichment in *Parabacteroides* was described after *in vitro* fermentation of xanthan gum using stools collected from mice with colitis (Zhang et al., 2023). In our study, xanthan gum addition resulted in the down-regulation of several taxa, including genera *Dorea*, *Lachnospiraceae* UCG-001, *Eubacterium ventriosum* group, *Intestinibacter*, *Faecalibacterium*, *Ruminococcus*, and species *Dorea formicigenerans* and *Bacteroides dorei* (Fig. 2G).

Differentially abundant bacteria included relevant SCFA-producing microbes; considering the observed reduction of bacterial diversity, it is tempting to speculate that changes in microbial communities due to xanthan–induced disturbance may directly affect ecosystem processes. Our results align with those of Naimi and co-workers, who reported a significant augmentation of the human microbiota with pro-inflammatory potential after *in vitro* fermentation of xanthan gum (Naimi et al., 2021).

3.4. Multiomics integration between fecal metabolomics and microbiota associated with gum supplementation

The results for the mixomics integration of metabolomics and metagenomics datasets by DIABLO modeling are displayed in Fig. 3. The results show a high correlation between the metabolomics dataset and the different taxa derived from metagenomics, either at family, genus and species levels, presenting the following correlation coefficients: 0.94, 0.94, and 0.93, respectively (Fig. 3A). Moreover, the Circos plot, including the connections between the different datasets, according to the significantly different variables, shows a deep interconnection between fermented metabolites and metagenomics datasets (correlation coefficient cut-off = 0.7; Fig. S2), thus indicating a clear interaction between fermentation-derived metabolites and the fecal microbiota. According to the effect of gum supplementation, the correlation heatmap derived from the DIABLO model indicates that xanthan gum provides a specific and exclusive impact on both the metabolomics and gut microflora, whereas the rest of the gums showed a more similar outcome among them, especially in the case of guar and locust bean gums, whereas gellan gum showed a close outcome with respect to control (Fig. 3B). At a metabolic level, these results align with those described earlier by multivariate statistics (Fig. 1G and 1H), as xanthan was grouped apart from the rest of the gums, whereas gellan gum was the closest treatment to the control. In the same way, the results from the diversity of the gut microbial communities agree with the omics integration, highlighting the exclusive profile associated with xanthan and the association between gellan gum and control and guar and locust bean gums (Fig. 2A).

The critical variables from each dataset were further obtained and displayed in Fig. 3C–F for metabolomics and metagenomics datasets, i.e.: family, genera, and species, respectively. Concerning metabolomics, most of the critical features were attributed to xanthan gum, exhibiting an accumulation of lignans, such as 1-acetoxypinoresinol, 7-hydroxymatairesinol, and schisandrin B (Fig. 3C). The association between xanthan gum and lignans has been hypothesized in flaxseed-derived

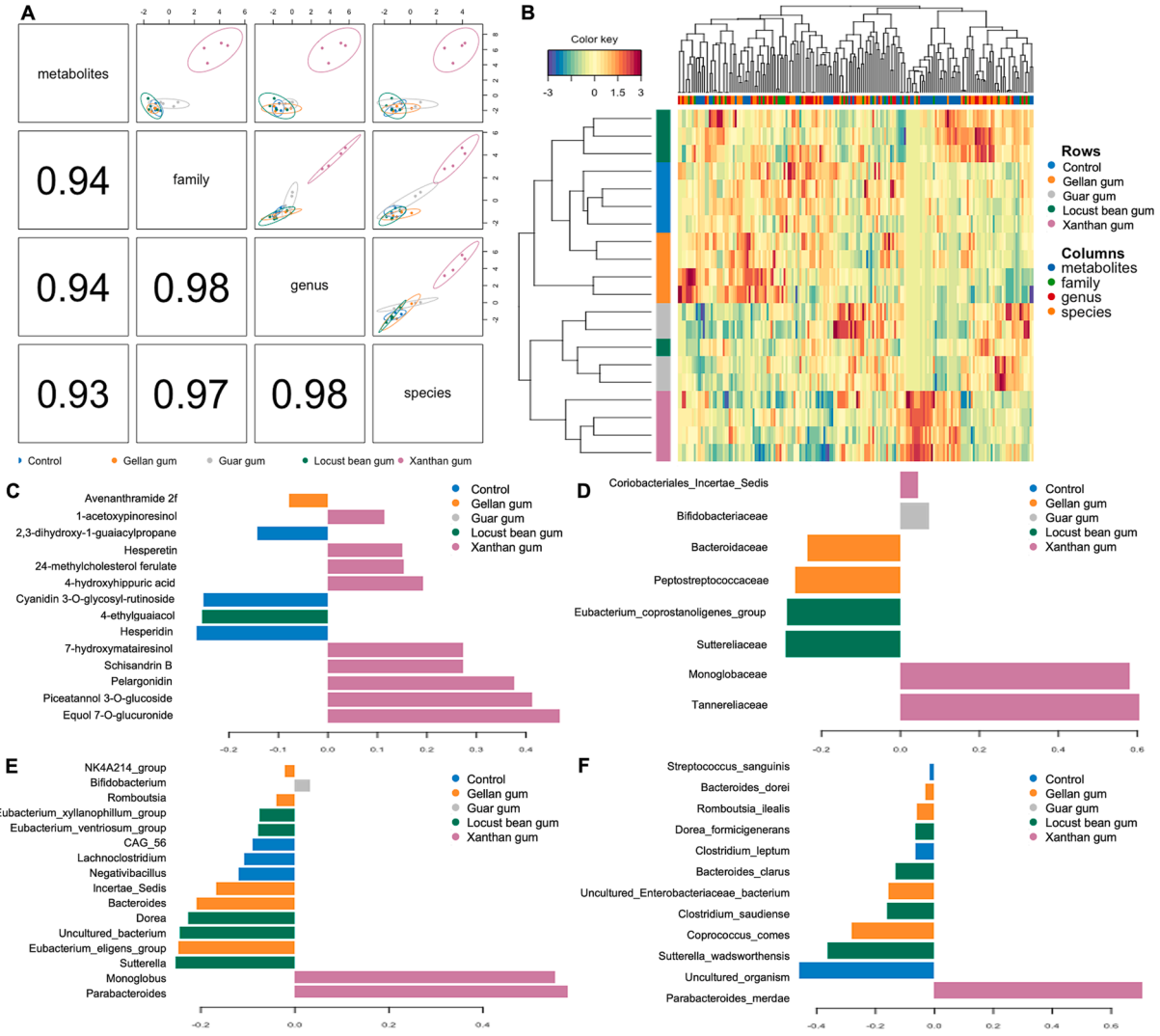

Fig. 3. DIABLO framework-derived mixomics integration. A. Correlation matrix comparing the four data blocks involved in the unique component of the DIABLO model. B. Heatmap-based correlation plot of most critical variables from both metabolomics and metagenomics datasets. C–F. Loading plots for the most discriminant features among treatments associated with omics dataset: metabolomics, metagenomics-derived family, metagenomics-derived genera, and metabolomics-derived species, respectively (all variables were found as critical by component 1).

preparations (Lee et al., 2021), suggesting a protective role of xanthan towards this family of compounds during *in vitro* digestion and fermentation. In contrast, the increased levels of flavonoid aglycones, represented by pelargonidin and hesperetin, and the polyphenol catabolites 4-hydroxy-hippuric acid, piceatannol 3-*O*-glucoside and equol 7-*O*-glucuronide attributed to xanthan gum (Fig. 3C), reveals that polyphenols were mainly metabolized by the gut microbiota assisted by this polysaccharide, due to the accumulation of these well-known catabolites (Carregosa et al., 2022).

Concerning the critical variables derived from gut microbiota metagenomics datasets (Fig. 3D–F), several synergies were found at all taxonomic levels associated with polysaccharidic gums. Unfortunately, restricted information is available concerning the enzymatic potential of human intestinal bacterial species associated with the conversion of polyphenols so as to establish a clear insight between the annotated fecal metabolites and gut microbiota distribution due to gum enrichment. In the case of gellan gum, a decrease in avenanthramide 2f levels coupled with a decrease in *B. dorei*, *R. ilealis*, and *Coprococcus comes* was spotted. The decrease in this metabolite could be due to its conversion to simpler metabolites, such as caffeic acid and ferulic acid, spotted as two major regulators of the gut microbiota (Yu et al., 2022). Interestingly, locust bean gum was associated with a decrease of 4-ethylguaiacol and reduced levels of several bacterial taxa in fecal samples. To the best of our knowledge, the ability of gut bacteria to produce guaiacol has been demonstrated only in insects following digestion of the plant material mediated by the decarboxylation of vanillic acid from lignin degradation (Dillon et al., 2000). Omics data integration reported the huge impact of xanthan gum supplementation, affecting both the fecal phenolic metabolome and gut microbiota modulation. Among class Bacteroidia, β-glucosidases and α-rhamnosidases involved in the deglycosylation of flavonoids have been identified in *Parabacteroides distasonis* (Goris et al., 2021), which is another former *Bacteroides* species close to *P. merdae*. In agreement with these results, *Tannerellaceae,* specifically genus *Parabacteroides,* have been implicated in the transformation of rhamnose glycosides such as rutin (Riva et al., 2020), being in agreement with the enhanced presence of flavonoid aglycones, such as hesperetin and pelargonidin (Fig. 3C), coupled with the enhanced presence of *P. merdae* (Fig. 3F) due to xanthan gum supplementation of *Aronia* puree. Despite numerous studies demonstrating the relationship between dietary polyphenols and gut microbiota, these interactions can be either direct or indirect, and dynamics can involve microbial metabolism of polyphenols as well as polyphenols modulation of the gut microbiota to stimulate or inhibit bacterial growth under the presence of polysaccharide fibers (García-Pérez et al., 2024). It is thus clear that further investigation will be needed to understand the intricate interplay between gut microorganisms and polyphenols and to clarify the biochemical mechanisms underlying the combined impact of dietary gums on this interaction.

4. Conclusions

The supplementation of different gums to *Aronia* puree affected the bioaccessibility of phenolics during *in vitro* gastrointestinal digestion and fermentation, as well as the human gut microbiota profile. The supplementation of locust bean gum promoted a significant increase in the bioaccessibility of low-molecular-weight phenolics after digestion and phenolic acids after either digestion or fermentation steps, being mostly represented by gallic acid, ferulic acid, and *p*-coumaric acid and derivatives. In the same way, the application of metagenomics revealed a gum-dependent effect on the gut microbiota, significantly impacting health-related bacterial groups. Among them, locust bean gum promoted a general accumulation of short-chain fatty acid-producing bacteria belonging to *Roseburia*, *Ruminococcus*, and *Lachnospiraceae.* The application of multi-omics integrative approaches suggests a double-edged effect of gum supplementation on fermented phenolic metabolites composition and the distribution of the gut microbiota populations, thus affecting the bioaccessibility of *Aronia* polyphenols. Given these findings, further research to get a clear outcome about the impact of polysaccharide gum supplementation on gut health *in vivo* is warranted. The development of dietary fiber-enriched functional foods opens up new possibilities for the food industry to design and produce foods with presumably health-related benefits. Therefore, it is important to better understand the effects and action mechanism of these interactions and the fate of polyphenol bioaccessibility to drive concrete conclusions for future functional food studies.

CRediT authorship contribution statement

Merve Tomas: Conceptualization, Formal analysis, Investigation, Methodology, Resources, Visualization, Writing – original draft, Writing – review & editing. **Pascual García-Pérez:** Formal analysis, Investigation, Methodology, Visualization, Writing – original draft, Writing – review & editing. **Araceli Rivera-Pérez:** Methodology, Visualization, Writing – review & editing. **Vania Patrone:** Formal analysis, Investigation, Resources, Visualization, Writing – original draft, Writing – review & editing. **Gianluca Giuberti:** Investigation, Resources, Writing – original draft, Writing – review & editing. **Luigi Lucini:** Investigation, Project administration, Supervision, Writing – review & editing. **Esra Capanoglu:** Conceptualization, Formal analysis, Investigation, Methodology, Project administration, Writing – original draft, Writing – review & editing.

Declaration of Competing Interest

The authors declare that they have no known competing financial interests or personal relationships that could have appeared to influence the work reported in this paper.

Data availability

Data are attached as supplementary material

Acknowledgements

P.G.-P. thanks the “Margarita Salas” postdoctoral grant supported by the European Union through the “NextGenerationEU” program, provided by the University of Vigo. A.R.-P. acknowledges the Grant FPU18/05133 awarded by the Spanish University’s Ministry. The authors also thank the “Romeo ed Enrica Invernizzi” foundation (Milan, Italy) for supporting the metabolomics facilities at the Università Cattolica del Sacro Cuore.

Appendix A. Supplementary material

Supplementary data to this article can be found online at https://doi.org/10.1016/j.foodchem.2023.138231.

References

Abu Elella, M. H., Goda, E. S., Gab-Allah, M. A., Hong, S. E., Pandit, B., Lee, S., Gamal, H., Rehman, A. U., & Yoon, K. R. (2021). Xanthan gum-derived materials for applications in environment and eco-friendly materials: A review. *Journal of Environmental Chemical Engineering, 9*(1), Article 104702. https://doi.org/10.1016/j.jece.2020.104702

Al-Lahham, S. H., Peppelenbosch, M. P., Roelofsen, H., Vonk, R. J., & Venema, K. (2010). Biological effects of propionic acid in humans; metabolism, potential applications and underlying mechanisms. *Biochimica et Biophysica Acta - Molecular and Cell Biology of Lipids, 1801*(11), 1175–1183. https://doi.org/10.1016/j.bbalip.2010.07.007

Apak, R., Güçlü, K., Özyürek, M., & Karademir, S. E. (2004). Novel total antioxidant capacity index for dietary polyphenols and vitamins C and E, using their cupric ion reducing capability in the presence of neocuproine: CUPRAC method. *Journal of Agricultural and Food Chemistry, 52*(26), 7970–7981. https://doi.org/10.1021/jf048741x

Capanoglu, E., Beekwilder, J., Boyacioglu, D., Hall, R., & de Vos, R. (2008). Changes in antioxidant and metabolite profiles during production of tomato paste. *Journal of Agricultural and Food Chemistry, 56*(3), 964–973. https://doi.org/10.1021/jf072990e

Carregosa, D., Pinto, C., Ávila-Gálvez, M.Á., Bastos, P., Berry, D., & Santos, C. N. (2022). A look beyond dietary (poly)phenols: The low molecular weight phenolic metabolites and their concentrations in human circulation. In *Comprehensive reviews in food science and food safety*. https://doi.org/10.1111/1541-4337.13006

Castro-Alves, V. C., & Cordenunsi, B. R. (2015). Total soluble phenolic compounds quantification is not as simple as it seems. *Food Analytical Methods, 8*(4), 873–884. https://doi.org/10.1007/s12161-014-9961-0

Chen, J., Wright, K., Davis, J. M., Jeraldo, P., Marietta, E. V., Murray, J., Nelson, H., Matteson, E. L., & Taneja, V. (2016). An expansion of rare lineage intestinal microbes characterizes rheumatoid arthritis. *Genome Medicine, 8*(1), 1–14. https://doi.org/10.1186/s13073-016-0299-7

Das, M., & Giri, T. K. (2020). Hydrogels based on gellan gum in cell delivery and drug delivery. *Journal of Drug Delivery Science and Technology*, *56*(December 2019), 101586. 10.1016/j.jddst.2020.101586.

Dey, E. S., Ahmadi-Afzadi, M., Nybom, H., & Tahir, I. (2013). Alkylresorcinols isolated from rye bran by supercritical fluid of carbon dioxide and suspended in a food-grade emulsion show activity against *Penicillium expansum* on apples. *Archives of Phytopathology and Plant Protection, 46*(1), 105–119. https://doi.org/10.1080/03235408.2012.734719

Dillon, R. J., Vennard, C. T., & Charnley, A. K. (2000). Exploitation of gut bacteria in the locust. *Nature, 403*(6772), 851. https://doi.org/10.1038/35002669

Do, M. H., Lee, H. H. L., Lee, J. E., Park, M., Oh, M. J., Lee, H. Bin, Park, J. H., Jhun, H., Kim, J. H., Kang, C. H., & Park, H. Y. (2023). Gellan gum prevents non-alcoholic fatty liver disease by modulating the gut microbiota and metabolites. *Food Chemistry*, *400*(August 2022), 134038. 10.1016/j.foodchem.2022.134038.

Everette, J. D., Bryant, Q. M., Green, A. M., Abbey, Y. A., Wangila, G. W., & Walker, R. B. (2010). Thorough study of reactivity of various compound classes toward the folin−Ciocalteu reagent. *Journal of Agricultural and Food Chemistry, 58*(14), 8139–8144. https://doi.org/10.1021/jf1005935

Fettig, N. M., Robinson, H. G., Allanach, J. R., Davis, K. M., Simister, R. L., Wang, E. J., Sharon, A. J., Ye, J., Popple, S. J., Seo, J. H., Gibson, D. L., Crowe, S. A., Horwitz, M. S., & Osborne, L. C. (2022). Inhibition of Th1 activation and differentiation by dietary guar gum ameliorates experimental autoimmune encephalomyelitis. *Cell Reports, 40*(11), Article 111328. https://doi.org/10.1016/j.celrep.2022.111328

García-Pérez, P., Tomas, M., Rivera-Pérez, A., Patrone, V., Giuberti, G., Cervini, M., Capanoglu, E., & Lucini, L. (2024). Pectin conformation influences the bioaccessibility of cherry laurel polyphenols and gut microbiota distribution following in vitro gastrointestinal digestion and fermentation. *Food Chemistry, 430*, 2023). https://doi.org/10.1016/j.foodchem.2023.137054

Goris, T., Cuadrat, R. R. C., & Braune, A. (2021). Flavonoid-modifying capabilities of the human gut microbiome—An in silico study. *Nutrients, 13*(8). https://doi.org/10.3390/nu13082688

Grgić, J., Šelo, G., Planinić, M., Tišma, M., & Bucić-Kojić, A. (2020). Role of the encapsulation in bioavailability of phenolic compounds. *Antioxidants, 9*(10), 1–36. https://doi.org/10.3390/antiox9100923

Isaías, R., Frias, A., Rocha, C., Moura, A. P., & Cunha, L. M. (2023). *Chapter 15 - Designing and development of food structure with high acceptance based on the consumer perception*. In M. Â. P. R. Cerqueira & L. M. B. T.-F. S. E. and D. for I. N. Pastrana Castro Health and Well-Being (eds.); pp. 399–414). Academic Press. 10.1016/B978-0-323-85513-6.00013-X.

Jakobek, L., Ištuk, J., Tomac, I., & Matić, P. (2022). β-Glucan and aronia (aronia melanocarpa) phenolics: Interactions during in vitro simulated gastrointestinal digestion and adsorption. *Polish Journal of Food and Nutrition Sciences, 72*(4), 371–380. https://doi.org/10.31883/pjfns/155281

Kim, C. C., Healey, G. R., Kelly, W. J., Patchett, M. L., Jordens, Z., Tannock, G. W., Sims, I. M., Bell, T. J., Hedderley, D., Henrissat, B., & Rosendale, D. I. (2019). Genomic insights from Monoglobus pectinilyticus: A pectin-degrading specialist bacterium in the human colon. *ISME Journal, 13*(6), 1437–1456. https://doi.org/10.1038/s41396-019-0363-6

Lee, C. G., Shim, Y. Y., Reaney, M. J. T., & Chang, H. J. (2021). Food puree for seniors: The effects of xanflax as a new thickener on physicochemical and antioxidant properties. *Foods, 10*(5), 1–10. https://doi.org/10.3390/foods10051100

Lee, J., Durst, R. W., & Wrolstad, R. E. (2005). Determination of total monomeric anthocyanin pigment content of fruit juices, beverages, natural colorants, and wines by the pH differential method: Collaborative study. *Journal of AOAC International, 88*(5), 1269–1278. https://doi.org/10.1093/jaoac/88.5.1269

Lenoir, M., Martín, R., Torres-Maravilla, E., Chadi, S., González-Dávila, P., Sokol, H., Langella, P., Chain, F., & Bermúdez-Humarán, L. G. (2020). Butyrate mediates anti-inflammatory effects of Faecalibacterium prausnitzii in intestinal epithelial cells through Dact3. *Gut Microbes, 12*(1), 1–16. https://doi.org/10.1080/19490976.2020.1826748

Li, J., Wu, T., Li, N., Wang, X., Chen, G., & Lyu, X. (2019). Bilberry anthocyanin extract promotes intestinal barrier function and inhibits digestive enzyme activity by regulating the gut microbiota in aging rats. *Food and Function, 10*(1), 333–343. https://doi.org/10.1039/c8fo01962b

Liu, X., Renard, C. M. G. C., Rolland-Sabaté, A., & Le Bourvellec, C. (2021). Exploring interactions between pectins and procyanidins: Structure-function relationships. *Food Hydrocolloids, 113*, 2020. https://doi.org/10.1016/j.foodhyd.2020.106498

Loo, Y. T., Howell, K., Suleria, H., Zhang, P., Liu, S., & Ng, K. (2023). Fibre fermentation and pig faecal microbiota composition are affected by the interaction between sugarcane fibre and (poly) phenols in vitro. *International Journal of Food Sciences and Nutrition*, 1–15. https://doi.org/10.1080/09637486.2023.2187329

Ma, L., Ni, Y., Wang, Z., Tu, W., Ni, L., Zhuge, F., Zheng, A., Hu, L., Zhao, Y., Zheng, L., & Fu, Z. (2020). Spermidine improves gut barrier integrity and gut microbiota function in diet-induced obese mice. *Gut Microbes, 12*(1), 1–19. https://doi.org/10.1080/19490976.2020.1832857

Minekus, M., Alminger, M., Alvito, P., Ballance, S., Bohn, T., Bourlieu, C., Carrière, F., Boutrou, R., Corredig, M., Dupont, D., Dufour, C., Egger, L., Golding, M., Karakaya, S., Kirkhus, B., Le Feunteun, S., Lesmes, U., Macierzanka, A., Mackie, A., & Brodkorb, A. (2014). A standardised static in vitro digestion method suitable for food – an international consensus. *Food & Function, 5*(6), 1113–1124. https://doi.org/10.1039/C3FO60702J

Miragoli, F., Patrone, V., Prandini, A., Sigolo, S., Dell'anno, M., Rossi, L., Senizza, A., Morelli, L., & Callegari, M. L. (2021). Implications of tributyrin on gut microbiota shifts related to performances of weaning piglets. *Microorganisms, 9*(3), 1–15. https://doi.org/10.3390/microorganisms9030584

Mudgil, D., & Barak, S. (2019). *Chapter 2 - Classification, Technological Properties, and Sustainable Sources* (C. M. B. T.-D. F. P. Galanakis Recovery, and Applications (Ed.); pp. 27–58). Academic Press. 10.1016/B978-0-12-816495-2.00002-2.

Naimi, S., Viennois, E., Gewirtz, A. T., & Chassaing, B. (2021). Direct impact of commonly used dietary emulsifiers on human gut microbiota. *Microbiome, 9*(1), 1–19. https://doi.org/10.1186/s40168-020-00996-6

Patrone, V., Minuti, A., Lizier, M., Miragoli, F., Lucchini, F., Trevisi, E., Rossi, F., & Callegari, M. L. (2018). Differential effects of coconut versus soy oil on gut microbiota composition and predicted metabolic function in adult mice. *BMC Genomics, 19*(1), 1–18. https://doi.org/10.1186/s12864-018-5202-z

Pérez-Burillo, S., Molino, S., Navajas-Porras, B., Valverde-Moya, Á. J., Hinojosa-Nogueira, D., López-Maldonado, A., Pastoriza, S., & Rufián-Henares, J.Á. (2021). An in vitro batch fermentation protocol for studying the contribution of food to gut microbiota composition and functionality. *Nature Protocols, 16*(7), 3186–3209. https://doi.org/10.1038/s41596-021-00537-x

Riva, A., Kolimár, D., Spittler, A., Wisgrill, L., Herbold, C. W., Abrankó, L., & Berry, D. (2020). Conversion of rutin, a prevalent dietary flavonol, by the human gut microbiota. *Frontiers in Microbiology, 11*(December), 1–11. https://doi.org/10.3389/fmicb.2020.585428

Rainero, G., Bianchi, F., Rizzi, C., Cervini, M., Giuberti, G., & Simonato, B. (2022). Breadstick fortification with red grape pomace: Effect on nutritional, technologial and sensory properties. *Journal of the Science of Food and Agriculture, 102*(6), 2545–2552. https://doi.org/10.1002/jsfa.11596

Rocchetti, G., Gregorio, R. P., Lorenzo, J. M., Barba, F. J., Oliveira, P. G., Prieto, M. A., Simal-Gandara, J., Mosele, J. I., Motilva, M. J., Tomas, M., Patrone, V., Capanoglu, E., & Lucini, L. (2022). Functional implications of bound phenolic compounds and phenolics–food interaction: A review. *Comprehensive Reviews in Food Science and Food Safety, 21*(2), 811–842. https://doi.org/10.1111/1541-4337.12921

Sapper, M., Talens, P., & Chiralt, A. (2019). Improving functional properties of cassava starch-based films by incorporating xanthan, gellan, or pullulan gums. *International Journal of Polymer Science, 2019*(6), 1–9. https://doi.org/10.1155/2019/5367164

Sidor, A., & Gramza-Michałowska, A. (2019). Black chokeberry *Aronia melanocarpa* L.—A qualitative composition, phenolic profile and antioxidant potential. *Molecules, 24*, 3710. https://doi.org/10.3390/molecules24203710

Singleton, V. L., & Rossi, J. A. (1965). Colorimetry of Total Phenolics with Phosphomolybdic-Phosphotungstic Acid Reagents. *American Journal of Enology and Viticulture, 16*(3), 144 LP–158. http://www.ajevonline.org/content/16/3/144.abstract.

Thomson, C., Garcia, A. L., & Edwards, C. A. (2021). Interactions between dietary fibre and the gut microbiota. *Proceedings of the Nutrition Society, 80*(4), 398–408. https://doi.org/10.1017/S0029665121002834

Tomas, M. (2022). Effect of dietary fiber addition on the content and in vitro bioaccessibility of antioxidants in red raspberry puree. *Food Chemistry*, *375*(June 2021), 131897. 10.1016/j.foodchem.2021.131897.

Tomas, M., Rocchetti, G., Ghisoni, S., Giuberti, G., Capanoglu, E., & Lucini, L. (2020). Effect of different soluble dietary fibres on the phenolic profile of blackberry puree subjected to in vitro gastrointestinal digestion and large intestine fermentation. *Food Research International*, *130*(September 2019). 10.1016/j.foodres.2019.108954.

Viuda-Martos, M., Lucas-Gonzalez, R., Ballester-Costa, C., Pérez-Álvarez, J. A., Muñoz, L. A., & Fernández-López, J. (2018). Evaluation of protective effect of different dietary fibers on polyphenolic profile stability of maqui berry (Aristotelia chilensis (Molina) Stuntz) during in vitro gastrointestinal digestion. *Food and Function, 9*(1), 573–584. https://doi.org/10.1039/c7fo01671a

Widelska, G., Wójtowicz, A., Kasprzak, K., Dib, A., Oniszczuk, T., Olech, M., Wojtunik-Kulesza, K., Nowak, R., Sujak, A., Dobrzański, B., & Oniszczuk, A. (2019). Impact of xanthan gum addition on phenolic acids composition and selected properties of new gluten-free maize-field bean pasta. *Open Chemistry, 17*(1), 587–598. https://doi.org/10.1515/chem-2019-0075

Wu, L. T., Tsai, I. L., Ho, Y. C., Hang, Y. H., Lin, C., Tsai, M. L., & Mi, F. L. (2021). Active and intelligent gellan gum-based packaging films for controlling anthocyanins release and monitoring food freshness. *Carbohydrate Polymers*, *254*(June 2020), 117410. 10.1016/j.carbpol.2020.117410.

Yu, Y., Zhou, L., Li, X., Liu, J., Li, H., Gong, L., Zhang, J., Wang, J., & Sun, B. (2022). The progress of nomenclature, structure, metabolism, and bioactivities of oat novel phytochemical: Avenanthramides. *Journal of Agricultural and Food Chemistry, 70*(2), 446–457. https://doi.org/10.1021/acs.jafc.1c05704

Zhang, S., Sun, Y., Nie, Q., Hu, J., Su, W., Guo, Z., Zhang, Y., & Nie, S. (2023). In vitro assessment of the effect of four polysaccharides on intestinal bacteria of mice with colitis. *Food Frontiers, May*, 1–10. https://doi.org/10.1002/fft2.270

Zhao, L., Pan, F., Mehmood, A., Zhang, H., Ur Rehman, A., Li, J., Hao, S., & Wang, C. (2021). Improved color stability of anthocyanins in the presence of ascorbic acid

with the combination of rosmarinic acid and xanthan gum. *Food Chemistry, 351* (January), Article 129317. https://doi.org/10.1016/j.foodchem.2021.129317